Bioorganic & Medicinal Chemistry 20 (2012) 3233–3241

Contents lists available at SciVerse ScienceDirect

Bioorganic & Medicinal Chemistry

journal homepage: www.elsevier.com/locate/bmc

Synthesis, biological evaluation, and molecular docking studies of 2,6-dinitro-4-(trifluoromethyl)phenoxysalicylaldoxime derivatives as novel antitubulin agents

Ting-Ting Zhao [a,†], Xiang Lu [a,†], Xian-Hui Yang [a], Li-Ming Wang [a], Xi Li [a], Zhong-Chang Wang [a], Hai-Bin Gong [b,*], Hai-Liang Zhu [a,*]

[a] State Key Laboratory of Pharmaceutical Biotechnology, Nanjing University, Nanjing 210093, PR China
[b] Xuzhou Central Hospital, Xuzhou 221009, PR China

ARTICLE INFO

Article history:
Received 23 February 2012
Revised 23 March 2012
Accepted 24 March 2012
Available online 1 April 2012

Keywords:
2* 6-Dinitro-4-(trifluoromethyl)phenoxysalicylaldoxime derivatives
Antitubulin polymerization
Structure–activity relationship
Molecular docking

ABSTRACT

A series of 2,6-dinitro-4-(trifluoromethyl)phenoxysalicylaldoxime derivatives (**1h–20h**) have been designed and synthesized, and their biological activities were also evaluated as potential antiproliferation and tubulin polymerization inhibitors. Among all the compounds, **2h** showed the most potent activity in vitro, which inhibited the growth of MCF-7, Hep-G2 and A549 cell lines with IC_{50} values of 0.70 ± 0.05, 0.68 ± 0.02 and 0.86 ± 0.05 μM, respectively. Compound **2h** also exhibited significant tubulin polymerization inhibitory activity (IC_{50} = 3.06 ± 0.05 μM). The result of flow cytometry (FCM) demonstrated that compound **2h** induced cell apoptosis. Docking simulation was performed to insert compound **2h** into the crystal structure of tubulin at colchicine binding site to determine the probable binding model. Based on the preliminary results, compound **2h** with potent inhibitory activity in tumor growth may be a potential anticancer agent.

1. Introduction

In conjunction with the spread of cardiovascular disease, cancer is today amongst the worldwide health threats.[1] Much work provided insights into the mechanisms of cancer and the antimitotic agents were widely used to treat human cancers.[2–4] Antimitotic agents cause mitotic arrest in eukaryotic cells by interfering with the polymerization–depolymerization process of tubulin dimmers of microtubule. Actually, blocking cell division by affecting the mitotic spindle has historically been a successful area of research for the advancement of cancer drugs.[5,6]

Classic antimitotic agents, many of which are tubulin-binding agents, such as colchicines[6–10] taxanes[9] and vinca alkaloids,[11] inhibit tubulin polymerization or interfere with microtubule disassembly, disrupting the dynamic equilibrium and then leading to cell cycle arrest or cell apoptosis. Apart from the above antimitotic agents, several other new compounds (Figs. 1 and 2), esp. compound **A** sharing the similar part with 2,6-dinitro-4-(trifluoromethyl)phenoxysalicylaldoxime derivatives, were found to inhibit the polymerization of tubulin by binding to the colchicine site.[10,12–14]

Among these structures (**A**, **C, D, E**, and compound **1h**), Schiff's base (or oxime) is a promising skeleton that has shown the good antitubulin activity. Schiff's base (esp. oxime) displays a variety of biological activities, such as anti-cancer,[15,16] anti-inflammatory,[17] anti-tuberculosis,[18] anti-fungal,[19] activities, and as herbicide.[20] Their broad biological properties are largely due to the exocyclic –RC═N– bond. The introduction of substituents to the terminal bonds of Schiff's base remains an area of pharmacological interest to activate Schiff's base; by the way, the introduction of O or N is more significant, such as Zorubicin[14] (Fig. 1C).

The incorporation of 1,3-dinitro-5-(trifluoromethyl)benzene could contribute to the binding of target compounds with tubulin. For instance, trifluoromethyl possess lipophilicify to penetrate the cell membrane. Trifluoromethyl substituents on phenyl ring are of particular interest. The isosteric substitution of hydrogen by the strong electron-withdrawing effect of CF_3 groups may increase the lipophilicity and thus enhance the rate of cell penetration, which is a very important feature in drug delivery in vivo, referring to prokaryotic as well as eukaryotic cells.[21–23] The higher polarizability due to the C–F bond may give rise to new possibilities for binding to the receptor. Trifluoromethyl substitution can also influence pharmacokinetic and pharmacodynamic properties of the molecule.[24] Furthermore, two nitro substituents of compounds could form hydrogen bond with the amino hydrogen of tubulin, which led to enhance antiproliferation and inhibition of tubulin polymerization activities.[25,26]

* Corresponding authors. Tel.: +86 25 8359 2572; fax: +86 25 8359 2672.
E-mail address: zhuhl@nju.edu.cn (H.-L. Zhu).
† These two authors equally contributed to this paper.

0968-0896/$ - see front matter Crown Copyright © 2012 Published by Elsevier Ltd. All rights reserved.
http://dx.doi.org/10.1016/j.bmc.2012.03.057

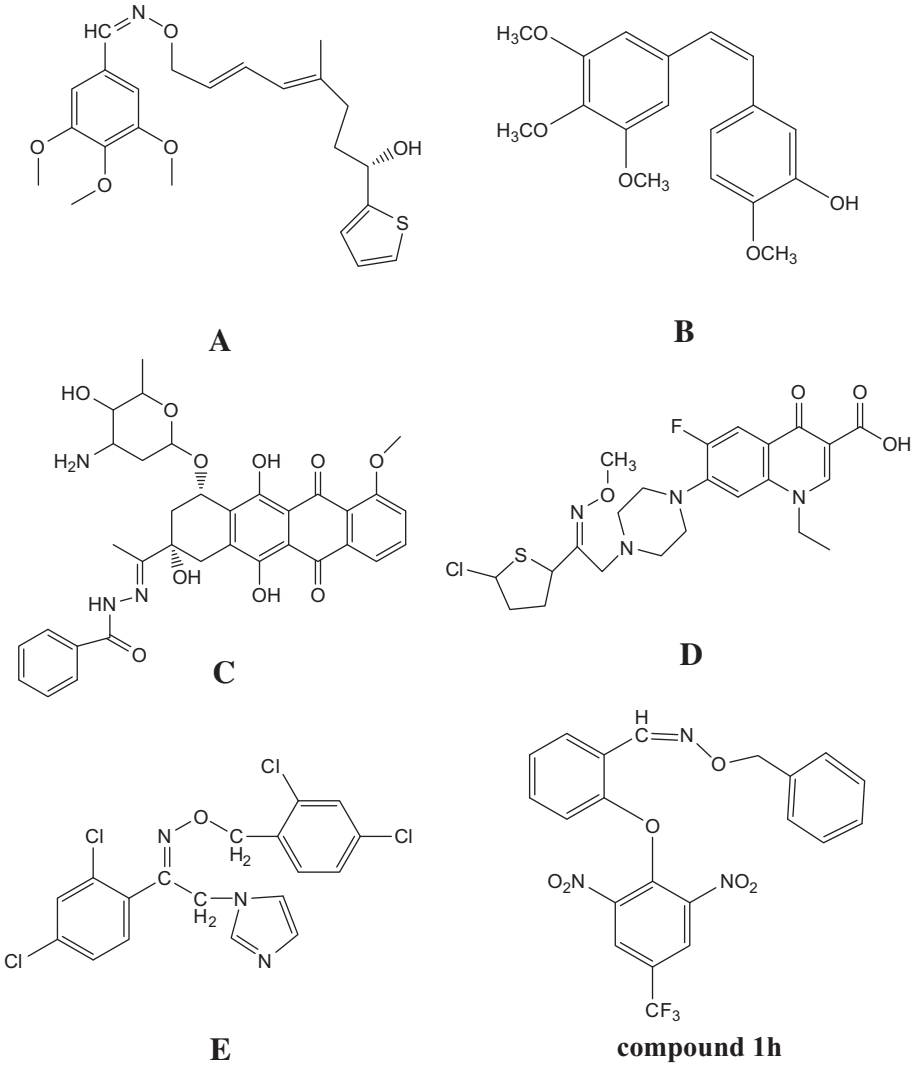

Figure 1. Chemical structures of antimitotic agents and lead tubulin inhibitors.

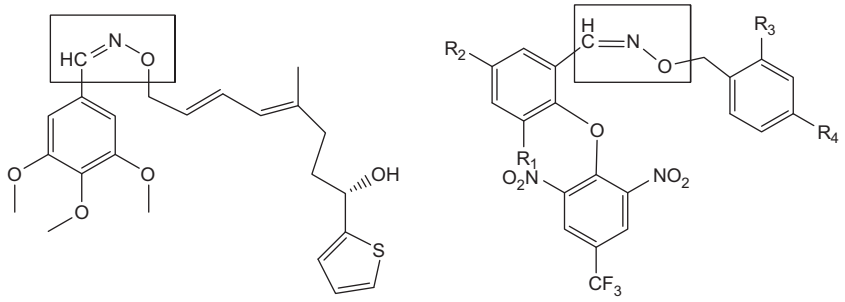

Figure 2. Similar part of compound **A** and 2,6-dinitro-4-(trifluoromethyl)phenoxysalicylaldoxime derivatives.

These previous researches encouraged us to integrate 1,3-dinitro-5-(trifluoromethyl)benzene with Schiff's base (oxime) to screen new 2,6-dinitro-4-(trifluoromethyl)phenoxysalicylaldoxime as potential antitubulin agents. The two combined substructures might exhibit synergistic effect in anticancer activities. Herein we report the synthesis and bioactivities of a series of novel 2,6-dinitro-4-(trifluoromethyl)phenoxysalicylaldoxime derivatives possessing Schiff's base to mimic the reported antimitotic agents. Their antiproliferation and inhibition of tubulin polymerization activities were evaluated. Molecular modeling studies were consequently performed to understand tubulin–inhibitor interaction. The docking results confirmed that hydrogen bonding may contribute to the potent biological activities.

2. Results and discussion

2.1. Chemistry

The general reaction pathway for the synthesis of 2,6-dinitro-4-(trifluoromethyl)phenoxysalicylaldoxime derivatives (**1h–20h**) is

outlined in Scheme 1A–C. Firstly, the different substituted *O*-benzylhydroxylamine hydrochloride (compound **d**) were coupled with substituted salicylaldehyde to generate salicylaldoxime derivatives, using triethylamine (TEA) as the deacid reagent, in a high yield of 85–95%. Secondly, the different substituted salicylaldoxime were treated with 2-chloro-1,3-dinitro-5-(trifluoromethyl)benzene (compound **f**) to afford the desired compounds **1h–20h** (Table 1), using K_2CO_3 as the deacid reagent, with a yield of 60–90%. By the way, the general synthetic procedure of compounds **d** and **f** was prepared according to Scheme 1A–C. All of the target compounds **1h–20h** were reported for the first time, and gave satisfactory analytical and spectroscopic data. ^{1}H NMR and ESI-MS spectra were consistent with the assigned structures.

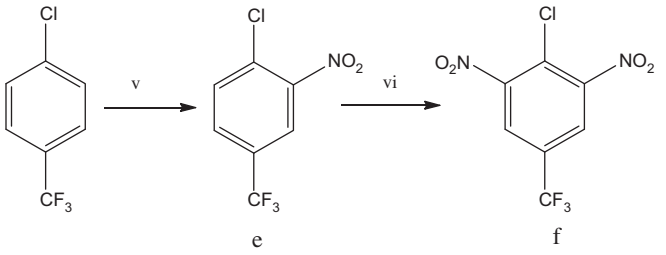

Scheme 1B. General synthesis of 2-chloro-1,3-dinitro-5-(trifluoromethyl)benzene (compounds **f**). Reagents and conditions: (v) HNO_3, H_2SO_4/SO_3, 50–70 °C, 2 h; (vi) HNO_3, H_2SO_4/SO_3, 100–115 °C, 2 h.

2.2. Crystal structure of compound

Among these compounds, a crystal structure of compound **4h** was determined by X-ray diffraction analysis. The crystal data are presented in Table 2 and Figure 3 give perspective views of **4h** with the atomic labeling system.

2.3. Bioactivity

2.3.1. Antiproliferative activities

The synthesized compounds were evaluated to test the antiproliferative activities against MCF-7, Hep-G2 and A549 cells. The results were summarized in Table 3. As shown in Table 3, these 2,6-dinitro-4-(trifluoromethyl)phenoxysalicylaldoxime derivatives bearing the Schiff moiety exhibited remarkable antiproliferative effects. Among them, compound **2h** displayed the most potent inhibitory activity (IC_{50} = 0.70 ± 0.05 μM for MCF-7, IC_{50} = 0.68 ± 0.02 μM for Hep-G2 and IC_{50} = 0.86 ± 0.05 μM for A549), comparable to the positive control combretastainA (CA-4) (IC_{50} = 0.41 ± 0.04 μM for MCF-7, IC_{50} = 0.19 ± 0.04 μM for Hep-G2, IC_{50} = 0.09 ± 0.01 μM for A549, respectively) and colchicine (IC_{50} = 0.53 ± 0.07 μM for MCF-7, IC_{50} = 0.23 ± 0.02 μM for Hep-G2, IC_{50} = 0.75 ± 0.08 μM for A549, respectively).

Subsequently, SAR (structure–activity relationships) studies were inferred from Table 3. In general, compounds without electron-withdrawing substituents showed more potent activities than those with them (halogen) in the A-ring (Table 1). Among the compounds of halogen substituents, the stronger and more electron-withdrawing effect, the lower antiproliferative activity. Therefore, Cl (**5h, 13h**) and Br (**9h, 17h**) group substituents had minimal effects compared with **1h**. Moreover, the position of substituents in the A-ring also influenced the activities owing to stereospecific blockade. For instance, *meta*-substituent in the A-ring of compounds (**13h**, **17h** etc.) would block the binding of nitro in the C-ring (Table 1) with the colchicine binding site of tubulin.

However, as for the B-ring (Table 1), inferred from Table 3, compounds (**2h, 3h**) with *ortho* and *para* electron-withdrawing substituents (halogen) showed more potent activities than those (**1h**) without them. Among the compounds of halogen substituents, the stronger and more electron-withdrawing effect, the higher antiproliferative activity and the strength order is F > Cl > H. That might be due to the high lipophilicity and metabolic stability of fluorine substituent. In other words, the presence of fluorine often leads to increased lipid solubility, thereby enhancing rates of absorption and transport of drugs in vivo.[27] Among all the compounds, **2h** displayed the best antiproliferative activity.

To examine whether the compounds interact with tubulin and inhibit tubulin polymerization in vitro, we performed the tubulin assembly assay. As shown in Table 3, some of these compounds showed strong inhibitory effect. Among them, compound **2h** (IC_{50} = 3.06 ± 0.05μM for tubulin) displayed the most potent anti-tubulin polymerization activity, comparable to the positive control (CA-4) (IC_{50} = 0.70 ± 0.20 μM for tubulin) and colchicine (IC_{50} = 1.72 ± 0.18 μM for tubulin). The results indicated the antiproliferative effect was produced by direct connection of tubulin and the compound.

2.3.2. Apoptosis assay

As representative of these 2,6-dinitro-4-(trifluoromethyl)phenoxysalicylaldoxime derivatives, compound **2h** has been under investigations in vitro experiment. We detected the mechanism of compound **2h** inhibition effect by flow cytometry (FCM) (Fig. 4), and found that the compound could induce the apoptosis of activated MCF-7 cells in a dose dependent manner. As shown

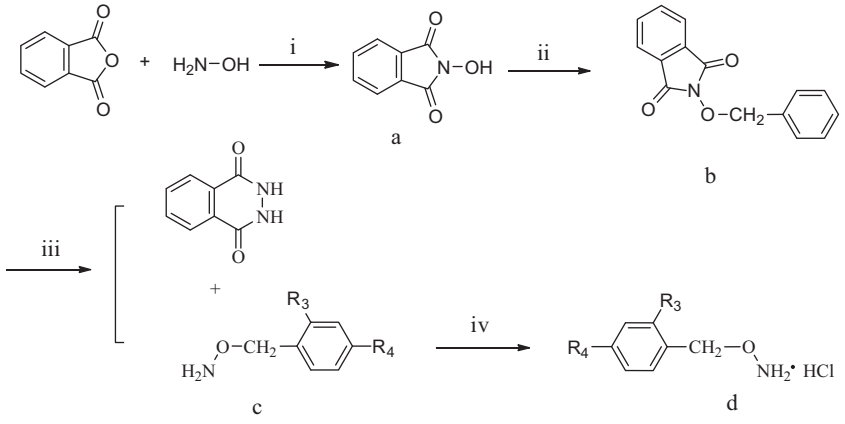

Scheme 1A. General synthesis of *O*-benzylhydroxylamine hydrochloride (compounds **d**). Reagents and conditions: (i) hydroxylamine, pyridine, 80 °C, overnight; (ii) Benzyl chloride, $NaHCO_3$, Bu_4NHSO_4, CH_2Cl_2/H_2O, reflux, 7 h; (iii) hydrazine hydrate, ethanol, rt, 1.5 h; (iv) CH_2Cl_2, HCl(g), rt, 1 h.

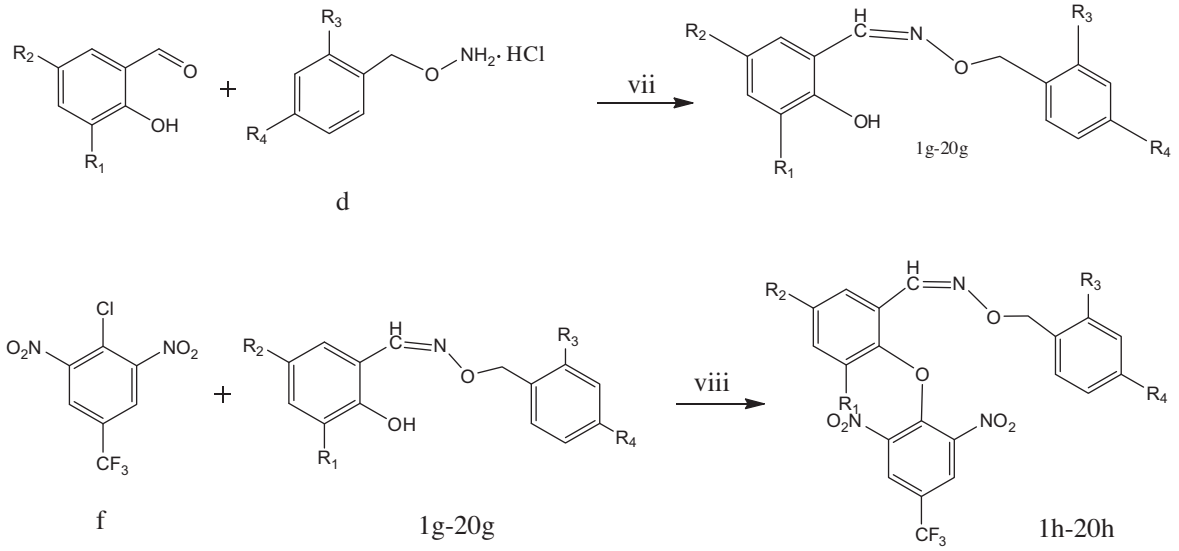

Scheme 1C. General synthesis of compounds **1h–20h**. Reagents and conditions: (vii) TEA, ethanol, rt, 0.5 h; (viii) 2-chloro-1,3-dinitro-5-(trifluoromethyl)benzene, K_2CO_3, DMF, 50–60 °C, 1 h.

Table 1
Structures of compounds **1h–20h**

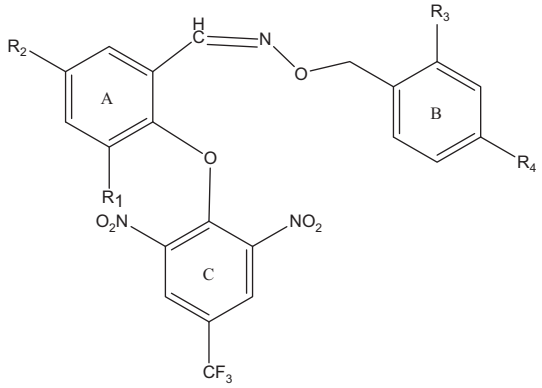

Compound	1h	2h	3h	4h	5h	6h	7h	8h	9h	10h
R1	H	H	H	H	H	H	H	H	H	H
R2	H	H	H	H	Cl	Cl	Cl	Cl	Br	Br
R3	H	F	Cl	Cl	H	F	Cl	Cl	H	F
R4	H	H	H	Cl	H	H	H	Cl	H	H
Compound	**11h**	**12h**	**13h**	**14h**	**15h**	**16h**	**17h**	**18h**	**19h**	**20h**
R1	H	H	Cl	Cl	Cl	Cl	Br	Br	Br	Br
R2	Br	Br	Cl	Cl	Cl	Cl	Br	Br	Br	Br
R3	Cl	Cl	H	F	Cl	Cl	H	F	Cl	Cl
R4	H	Cl	H	H	H	Cl	H	H	H	Cl

in Figure 4, MCF-7 cells were treated with 0, 0.01, 0.05, 0.25 μM of compound **2h** for 24 h. The compound increased the percentage of apoptosis by Annexin V-FITC/PI. The result indicated that compound **2h** could induce apoptosis of MCF-7 cells.

2.3.3. Binding model of compounds 2b into the colchicines binding site of tubulin

To gain better understanding on the potency of the studied compounds and guide further SAR studies, we proceeded to examine the interaction of compound **2h** with tubulin (PDB code: 1SA0). The molecular docking was performed by simulation of compound **2h** into the colchicine binding site of tubulin. All docking runs were

Table 2
Crystal data for compound **4h**

Crystal parameters	Compound **4h**
Formula	$C_{21}H_{12}Cl_2F_3N_3O_6$
Crystal size (mm)	0.2 × 0.2 × 0.1
MW (g mol^{-1})	530.24
Crystal system	Monoclinic
α(°)	90.00
β(°)	114.087(3)
γ(°)	90.00
a(Å)	12.530(5)
b(Å)	14.445(5)
c(Å)	13.827(5)
V(Å^3)	2284.9(15)
Z	30
θ limits(°)	$2.27 \leqslant \theta \leqslant 23.90$
hkl limits	$-14 \leqslant h \leqslant 14$, $-16 \leqslant k \leqslant 16$, $-15 \leqslant l \leqslant 15$
F(000)	1980
Data/restraints/parameters	3534/0/316
Absorption coefficient (mm^{-1})	1.177
Reflections collected	14072
Independent reflections	3534[R_{int} = 0.0475]
R_1 wR_2 [I>2&Gs(I)]	0.1157/0.3195
R_1 wR_2 (all data)	0.1661/0.3455
GOF	2.006

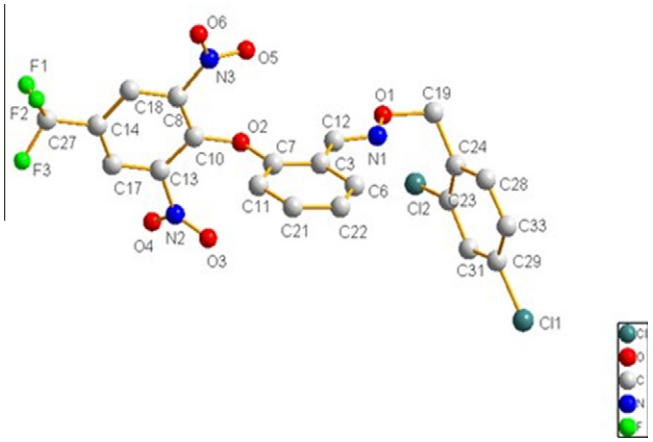

Figure 3. Crystal structure diagrams of compound **4h**.

Table 3
Inhibition (IC_{50}) of MCF-7, Hep-G2 and A549 cells proliferation and inhibition of tubulin polymerization by compounds **1h–20h**

Compound	IC_{50} ± SD (μM)			
	MCF-7[a]	Hep-G2[a]	A549[a]	Tubulin[b]
1h	1.33 ± 0.09	1.33 ± 0.17	1.47 ± 0.15	13.98 ± 0.93
2h	0.70 ± 0.05	0.68 ± 0.02	0.86 ± 0.05	3.06 ± 0.05
3h	1.1 ± 0.07	1.17 ± 0.12	1.43 ± 0.11	6.92 ± 0.53
4h	0.94 ± 0.11	1.02 ± 0.09	1.61 ± 0.07	4.08 ± 0.44
5h	1.22 ± 0.13	1.79 ± 0.07	3.41 ± 0.28	30.89 ± 2.16
6h	1.11 ± 0.08	1.02 ± 0.06	2.57 ± 0.06	7.07 ± 0.78
7h	3.95 ± 0.28	1.51 ± 0.14	5.03 ± 0.33	9.05 ± 0.81
8h	1.14 ± 0.13	1.28 ± 0.08	3.44 ± 0.29	7.54 ± 0.63
9h	1.15 ± 0.05	1.18 ± 0.15	2.24 ± 0.25	15.36 ± 0.97
10h	1.12 ± 0.07	0.89 ± 0.12	1.28 ± 0.03	6.90 ± 0.79
11h	2.84 ± 0.25	1.24 ± 0.02	3.43 ± 0.32	13.24 ± 1.02
12h	1.34 ± 0.08	1.07 ± 0.05	2.06 ± 0.19	7.06 ± 0.63
13h	1.21 ± 0.12	1.12 ± 0.07	1.45 ± 0.15	9.02 ± 0.93
14h	0.80 ± 0.09	0.82 ± 0.18	1.23 ± 0.02	3.65 ± 0.18
15h	1.96 ± 0.03	1.12 ± 0.24	2.16 ± 0.15	16.12 ± 1.07
16h	1.03 ± 0.09	0.94 ± 0.11	1.42 ± 0.04	6.18 ± 0.70
17h	1.83 ± 0.21	1.48 ± 0.13	2.15 ± 0. 26	18.01 ± 1.63
18h	0.88 ± 0.07	1.10 ± 0.08	1.56 ± 0.05	4.53 ± 0.08
19h	2.32 ± 0.14	2.45 ± 0.10	4.12 ± 0.43	18.09 ± 1.51
20h	2.09 ± 0.16	1.05 ± 0.10	6.19 ± 0.05	15.66 ± 1.24
CA-4	0.41 ± 0.04	0.19 ± 0.04	0.09 ± 0.01	0.70 ± 0.20
Colchicine	0.53 ± 0.07	0.23 ± 0.02	0.75 ± 0.08	1.72 ± 0.18

[a] Inhibition of the growth of tumor cell lines.
[b] Inhibition of tubulin polymerization.

applied LigandFit Dock protocol of Discovery Studio 3.1. The binding modes of compound **2h** and tubulin were depicted in Figure 5. All the amino acid residues which had interactions with tubulin were exhibited in Figure 5B. In the binding mode, compound **2h** was nicely bound to the colchicine binding site of tubulin by three hydrogen bonds. The oxygen atom of the hydroxyimino formed one hydrogen bond with the amino hydrogen of Asn C: 101 (N–H···O = 2.188 Å; 135.9°), the oxygen atom of the nitro groups on C-ring of **2h** formed another two hydrogen bonds with the amino hydrogen of Gly C: 144 (N–H···O = 1.732 Å; 147.5°) and Lys D254 (N–H···O = 2.154 Å; 116.3°), respectively. The 3D model of the interaction between compound **2h** and colchicin bonding site was showed in Figure 5A, which revealed that the molecule was well embedded in the active pocket, suggested that compound **2h** is a potential inhibitor of tubulin.

3. Conclusion

In our present work, a series of novel antitubulin polymerization inhibitors (**1h–20h**) have been firstly synthesized and evaluated. These compounds exhibited potent antiproliferative activities against MCF-7, Hep-G2 and A549 cells and tubulin polymerization inhibitory activity. Among them, compound **2h** demonstrated the most potent activity which inhibited the growth of MCF-7, Hep-G2 and A549 cells with IC_{50} values of 0.70 ± 0.05, 0.68 ± 0.02 and 0.86 ± 0.05 μM and inhibited the polymerization of tubulin with IC_{50} of 3.06 ± 0.05 μM. The result of flow cytometry (FCM) demonstrated that compound **2h** induced cell apoptosis.

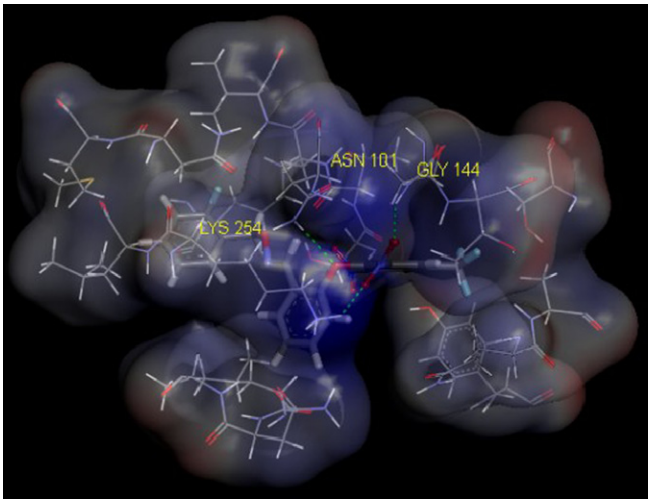

Figure 5A. The 3D model of the interaction between compound **2h** and colchicine bonding site. The protein is represented by molecular surface.

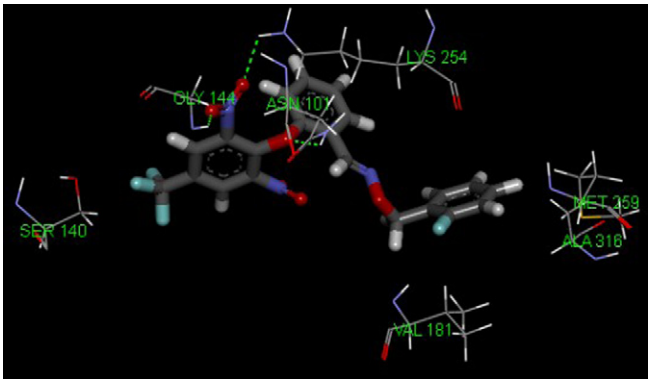

Figure 5B. The molecular docking of compound **2h** into tubulin. Compound **2h** (colored by atom: carbons: gray; nitrogen: blue; oxygen: red; chlorine: green) was nicely bound to the tubulin via three hydrogen bonds. (N–H···O = 2.188 Å; 135.9°. N–H···O = 1.732 Å; 147.5°. N–H···O = 2.154 Å; 116.3°.)

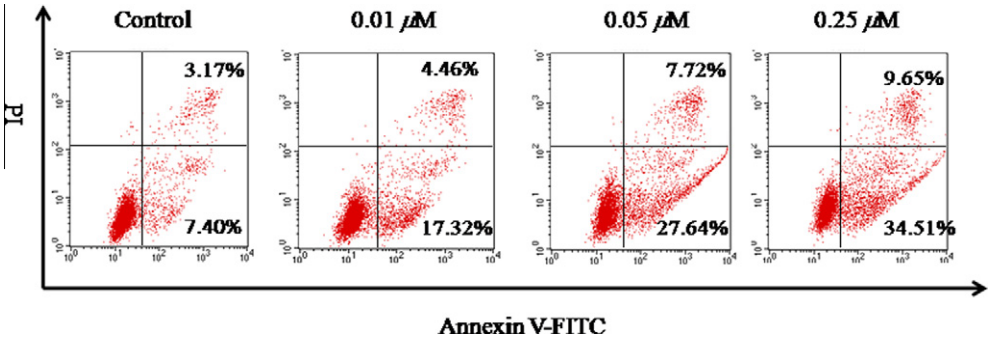

Figure 4. MCF-7 cells were cultured with various concentrations of compound **2h** for 24 h. Cells were stained by Annexin V-FITC/PI and apoptosis was analyzed by flow cytometry. Inhibition included early and late apoptosis.

Molecular docking showed that compound **2h** bound to the colchicines binding site by three hydrogen bond which might play a crucial role in its antitubulin polymerization and antiproliferative activities. This study might be helpful for the design and synthesis of tubulin polymerization inhibitors with stronger activities.

4. Experiments

4.1. Materials and measurements

All chemicals and reagents used in the current study were of analytical grade. Melting points (uncorrected) were determined on an XT4 MP apparatus (Taike Corp., Beijing, China). All the ^{1}H NMR spectra were recorded on a Bruker DPX300 model Spectrometer in DMSO-d_6 and chemical shifts were reported in ppm (δ). FT-IR spectra (KBr) were run on a Nexus 870 FT-IR spectrophotometer. ESI-MS spectra were recorded on a Mariner System 5304 Mass spectrometer. Elemental analyses were performed on a CHN-O-Rapid instrument. TLC was performed on the glassbacked silica gel sheets (Silica Gel 60 GF254) and visualized in UV light (254 nm).

4.2. Synthesis

4.2.1. General synthetic procedure of *O*-benzylhydroxylamine hydrochloride (d)

A mixture of substituted isobenzofuran-1,3-dione and hydroxylamine was dissolved in pyridine and stirred on 80 °C overnight. The reaction was monitored by TLC. The mixture was poured into water and the product was precipitated. Then it was washed with trichlormethane and dried over anhydrous $MgSO_4$, filtered and evaporated to gain compound **a**. After reaction of compound **a** with $NaHCO_3$, the mixture was basified to pH 8–9, added Bu_4NHSO_4 and Benzyl chloride, and refluxed 7 h. The product was extracted with CH_2Cl_2/H_2O, dried over anhydrous $MgSO_4$, filtered and evaporated to gain compound **b**. Then compound **b** was added into ethanol. After cooling down to 0 °C, hydrazine hydrate was dropped. The mixture was reacted and stirred for 1.5 h to get compound **c**. At last, compound **c** was dissolved in CH_2Cl_2, and dry HCl(g) was vented. After reacting 1 h, HCl(g) was blowed with N_2 and compound **d** was yielded.

4.2.2. General synthetic procedure of 2-chloro-1,3-dinitro-5-(trifluoromethyl) benzene (f)

A mixture of nitric acid and sulfur trioxide was poured into 1-chloro-4-(trifluoromethyl)benzene. And the reaction was run at 50–70 °C for 3 h. The product was extracted with ethyl acetate and saturated $NaHCO_3$, filtered and recrystallized from ethanol to gain compound **e**. Similarly, the same mixture was poured into compound **e**. Then, the reaction was run at 100–115 °C for 2 h to synthsis 2-chloro-1,3-dinitro-5-(trifluoromethyl)benzene (compound **f**).

4.2.3. General synthetic procedure of target compounds (1h–20h)

A mixture of substituted *O*-benzylhydroxylamine hydrochloride (1 equiv), TEA (1 equiv) and substituted salicylaldehyde (1 equiv) was dissolved in absolute ethanol and stirred for 0.5 h. The reaction was monitored by TLC. The precipitate was filtered and recrystallized from ethanol to gain salicylaldoxime (compounds **1g–20g**).

Then K_2CO_3 (2 equiv), substituted salicylaldoxime (1 equiv) and 2-chloro-1,3-dinitro-5-(trifluoromethyl)benzene (1 equiv) were mixed and dissolved in DMF and stirred on 50–60 °C for 1 h. The solvent was evaporated until no longer liquid outflow. The products were extracted with ethyl acetate. The extract was washed successively with saturated NaCl solution, and then dried over anhydrous Na_2SO_4, filtered and evaporated. Finally the precipitate was filtered and recrystallized from ethanol to yield **1h–20h**.

4.3. Spectral properties of 2,6-dinitro-4-(trifluoromethyl) phenoxysalicylaldoxime derivatives

4.3.1. 2-(2, 6-Dinitro-4-(trifluoromethyl) phenoxy) benzaldehyde *O*-benzyl oxime (1h)

Yellow solid, yield 75%, mp: 92–94 °C. IR (KBr, ν, cm^{-1}): 1544 (s, C=N); 1319 (s, NO_2); 1144 (s, C–O–C). ^{13}C NMR (300 MHz, $CDCl_3$, ppm): δ 160.7; 153.8 (CH=N); 144.6; 137.3; 132.8; 131.1; 128.8; 127.8; 126.8; 126.7; 126.6; 123.3; 122.4; 119.7; 76.9 (CH_2). ^{1}H NMR ($CDCl_3$, 300 MHz): 5.23 (s, 2H); 6.97 (d, J = 8.22 Hz, 1H); 7.21 (t, J = 7.59 Hz, 1H); 7.32–7.45 (m, 6H); 7.81 (t, J = 3.84 Hz, 1H); 8.51 (s, 1H); 8.93 (s, 2H). ESI-MS: 461.35 ($C_{21}H_{15}F_3N_3O_6$ [M+H]$^+$). Anal. Calcd for $C_{21}H_{14}F_3N_3O_6$: C, 54.67; H, 3.06; N, 9.11. Found: C, 54.74; H, 3.09; N, 9.13.

4.3.2. 2-(2,6-Dinitro-4-(trifluoromethyl)phenoxy)benzaldehyde *O*-(2-fluorobenzyl) oxime (2h)

Yellow solid, yield 78%, mp: 98–100 °C. IR (KBr, ν, cm^{-1}): 1543 (s, C=N); 1320 (s, NO_2); 1143 (s, C–O–C). ^{13}C NMR (300 MHz, $CDCl_3$, ppm): δ 162.5; 159.2; 154.2 (CH=N); 144.6; 139.7; 132.8; 131.1; 130.7; 130.6; 129.8; 128.3; 127.8; 126.8; 126.7; 124.6; 124.4; 123.9; 123.3; 122.3; 119.6; 115.4; 115.1; 70.1 (CH_2). ^{1}H NMR ($CDCl_3$, 300 MHz): 5.35 (d, J = 8.40 Hz, 2H); 6.50 (d, J = 8.22 Hz, 1H); 7.43 (t, J = 9.135 Hz, 1H); 7.17(t, J = 7.05 Hz, 2H); 7.23–7.27 (m, 1H); 7.28–7.36 (m, 1H); 7.48–7.52 (m, 1H); 7.94–7.97 (m, 1H); 8.45 (s, 2H); 8.58 (s, 1H). ESI-MS: 479.34 ($C_{21}H_{14}F_4N_3O_6$ [M+H]$^+$). Anal. Calcd for $C_{21}H_{13}F_4N_3O_6$: C, 52.62; H, 2.73; N, 8.77. Found: C, 52.52; H, 2.70; N, 8.73.

4.3.3. (*E*)-2-(2,6-Dinitro-4-(trifluoromethyl) phenoxy)benzaldehyde *O*-(2-chloro- benzyl) oxime (3h)

Yellow solid, yield 68%, mp: 141–142 °C. IR (KBr, ν, cm^{-1}): 1553 (s, C=N); 1320 (s, NO_2); 1155 (s, C–O–C). ^{13}C NMR (300 MHz, $CDCl_3$, ppm): δ 160.4; 152.8 (CH=N); 140.1; 137.9; 135.2; 133.5; 131.3; 128.9; 128.1; 127.3; 125.7; 121.7; 121.0; 120.4; 73.5 (CH_2). ^{1}H NMR ($CDCl_3$, 300 MHz): 6.50–6.53 (m, 1H); 7.14–7.23 (m, 1H); 7.23–7.27 (m, 1H); 7.27–7.29 (m, 2H); 7.30–7.32 (m, 2H); 7.39–7.42 (m, 1H); 7.51–7.54 (m, 1H); 7.87–7.97 (m, 1H); 8.46 (m, 2H); 8.63 (m, 1H). ESI-MS: 495.79 ($C_{21}H_{14}ClF_3N_3O_6$ [M+H]$^+$). Anal. Calcd for $C_{21}H_{13}ClF_3N_3O_6$: C, 50.87; H, 2.64; N, 8.48. Found: C, 50.78; H, 2.69; N, 8.63.

4.3.4. (*E*)-2-(2,6-Dinitro-4-(trifluoromethyl) phenoxy)benzaldehyde *O*-(2,4-dichlo-robenzyl) oxime (4h)

Light yellow solid, yield 67%, mp: 142–143 °C. IR (KBr, ν, cm^{-1}): 1545 (s, C=N); 1321 (s, NO_2); 1144 (s, C–O–C). ^{13}C NMR (300 MHz, $CDCl_3$, ppm): δ 154.2 (CH=N); 144.6; 134.0; 133.8; 132.8; 131.3; 130.4; 128.4; 127.9; 127.1; 126.8; 126.7; 124.6; 123.3; 122.1; 119.6; 112.8; 73.4 (CH_2). ^{1}H NMR ($CDCl_3$, 300 MHz): 5.35 (d, J = 7.02 Hz, 2H); 6.50–6.53 (m, 1H); 7.14–7.23 (m, 1H); 7.24–7.27 (m, 1H); 7.27–7.30 (m, 1H); 7.42 (d, J = 2.19 Hz, 1H); 7.46 (d, J = 8.25 Hz, 1H); 7.91–7.94 (m, 1H); 8.46 (s, 2H); 8.62 (s, 1H). ESI-MS: 530.24 ($C_{21}H_{13}Cl_2F_3N_3O_6$ [M+H]$^+$). Anal. Calcd for $C_{21}H_{12}Cl_2F_3N_3O_6$: C, 47.57; H, 2.28; N, 7.92. Found: C, 47.65; H, 2.31; N, 7.90.

4.3.5. 5-Chloro-2-(2,6-dinitro-4-(trifluoromethyl) phenoxy)benzaldehyde *O*-benzyl oxime (5h)

Yellow solid, yield 89%, mp: 143–146 °C. IR (KBr, ν, cm^{-1}): 1549 (s, C=N); 1318 (s, NO_2); 1149 (s, C–O–C). ^{13}C NMR (300 MHz, $CDCl_3$, ppm): δ 161.3; 154.8 (CH=N); 143.2; 137.6; 137.2; 133.8; 131.2; 129.1; 127.0; 124.6; 121.7; 120.8; 120.6; 118.4; 110.8; 75.4 (CH_2). ^{1}H NMR ($CDCl_3$, 300 MHz): 5.25 (s, 2H); 7.08 (d,

J = 9.03 Hz, 1H); 7.37–7.45 (m, 6H); 7.76 (d, *J* = 2.55 Hz, 1H); 8.47 (s, 1H); 8.94 (s, 2H); ESI-MS: 495.79 ($C_{21}H_{14}ClF_3N_3O_6$ $[M+H]^+$). Anal. Calcd for $C_{21}H_{13}ClF_3N_3O_6$: C, 50.87; H, 2.64; N, 8.48. Found: C, 50.79; H, 2.64; N, 8.43.

4.3.6. 5-Chloro-2-(2,6-dinitro-4-(trifluoromethyl) phenoxy)benzaldehyde *O*-(2-fluorobenzyl) oxime (6h)

Yellow solid, yield 78%, mp: 122–126 °C. IR (KBr, *v*, cm^{-1}): 1537 (s, C=N); 1323 (s, NO_2); 1156 (s, C–O–C). ^{13}C NMR (300 MHz, $CDCl_3$, ppm): *δ* 156.5; 154.7; 153.8 (CH=N); 142.9; 138.8; 132.2; 129.1; 127.5; 127.4; 127.3; 126.1; 125.9; 124.6; 123.9; 123.2; 121.5; 120.1; 114.9; 68.8 (CH_2). ^1H NMR ($CDCl_3$, 300 MHz): 5.29 (s, 2H); 7.08 (d, *J* = 8.97 Hz, 1H); 7.21–7.27 (m, 2H); 7.39–7.45 (m, 2H); 5.21 (t, *J* = 7.59 Hz, 1H); 7.76 (d, *J* = 2.76 Hz, 1H); 8.46 (s, 1H); 8.94 (s, 2H). ESI-MS: 513.78 ($C_{21}H_{13}ClF_4N_3O$ $[M+H]^+$). Anal. Calcd for $C_{21}H_{12}ClF_4N_3O_6$: C, 49.09; H, 2.35; N, 8.18. Found: C, 49.18; H, 2.33; N, 8.03.

4.3.7. 5-Chloro-2-(2,6-dinitro-4-(trifluoromethyl) phenoxy)benzaldehyde *O*-(2-chlorobenzyl) oxime (7h)

Yellow solid, yield 87%, mp: 159–160 °C. IR (KBr, *v*, cm^{-1}): 1546 (s, C=N); 1319 (s, NO_2); 1151 (s, C–O–C). ^{13}C NMR (300 MHz, $CDCl_3$, ppm): *δ* 160.2; 153.6 (CH=N); 140.3; 138.8; 134.3; 133.8; 130.4; 127.9; 127.1; 125.9; 121.6; 120.9; 120.5; 117.8; 110.5; 77.6 (CH_2). ^1H NMR ($CDCl_3$, 300 MHz): 5.39 (s, 2H); 6.45 (d, *J* = 8.79 Hz, 1H); 7.18–7.21 (m, 1H); 7.26–7.32 (m, 2H); 3.73 (t, *J* = 4.58 Hz, 1H); 7.50 (t, *J* = 6.17 Hz, 1H); 7.93 (d, *J* = 2.55 Hz, 1H); 8.47 (s, 2H); 8.53 (s, 1H). ESI-MS: 530.24 ($C_{21}H_{13}Cl_2F_3N_3O_6$ $[M+H]^+$). Anal. Calcd for $C_{21}H_{12}Cl_2F_3N_3O_6$: C, 47.57; H, 2.28; N, 7.92. Found: C, 47.49; H, 2.33; N, 7.84.

4.3.8. 5-Chloro-2-(2,6-dinitro-4-(trifluoromethyl) phenoxy)benzaldehyde *O*-(2,4-d ichlorobenzyl) oxime (8h)

Yellow solid, yield 75%, mp: 166–167 °C. IR (KBr, *v*, cm^{-1}): 1543 (s, C=N); 1320 (s, NO_2); 1151 (s, C–O–C). ^{13}C NMR (300 MHz, $CDCl_3$, ppm): *δ* 158.5; 153.8 (CH=N); 141.3; 139.8; 135.3; 134.6; 133.8; 130.9; 130.6; 129.7; 128.6; 127.3; 127.1; 125.4; 123.9; 122.3; 121.5; 120.1; 72.5 (CH_2). ^1H NMR ($CDCl_3$, 300 MHz): 6.45 (d, *J* = 8.97 Hz, 1H); 7.18–7.22 (m, 1H); 7.26–7.30 (m, 3H); 7.39–7.42 (m, 1H); 7.49–7.61(m, 1H); 7.93 (d, *J* = 0.15 Hz, 1H); 8.46 (s, 2H); 8.53 (s, 1H). ESI-MS: 564.68 ($C_{21}H_{12}Cl_3F_3N_3O_6$ $[M+H]^+$). Anal. Calcd for $C_{21}H_{11}Cl_3F_3N_3O_6$: C,44.67; H, 1.96; N, 7.44. Found: C,44.59; H, 1.93; N, 7.44.

4.3.9. 5-Bromo-2-(2,6-dinitro-4-(trifluoromethyl) phenoxy)benzaldehyde *O*-benzyl oxime (9h)

Yellow solid, yield 72%, mp: 130–139 °C. IR (KBr, *v*, cm^{-1}): 1536 (s, C=N); 1323 (s, NO_2); 1151 (s, C–O–C). ^{13}C NMR (300 MHz, $CDCl_3$, ppm): *δ* 158.9; 152.8 (CH=N); 141.3; 139.8; 137.3; 137.2; 130.7; 128.6; 127.5; 127.3; 127.0; 125.7; 122.3; 122.1; 118.4; 111.3; 77.6 (CH_2). ^1H NMR ($CDCl_3$, 300 MHz): 7.26 (d, *J* = 19.92 Hz, 2H); 6.70 (d, *J* = 8.76 Hz, 1H); 7.33–7.44 (m, 5H); 7.52–7.56 (m, 1H); 7.89 (d, *J* = 2.58 Hz, 1H); 8.46 (s, 1H); 8.93 (s, 2H). ESI-MS: 540.24 ($C_{21}H_{14}BrF_3N_3O_6$ $[M+H]^+$). Anal. Calcd for $C_{21}H_{13}BrF_3N_3O_6$: C, 46.69; H, 2.43; N, 7.78. Found: C, 46.77; H, 2.46; N, 7.73.

4.3.10. 5-Bromo-2-(2,6-dinitro-4-(trifluoromethyl) phenoxy)benzaldehyde *O*-(2- fluorobenzyl) oxime (10h)

Yellow solid, yield 82%, mp: 121–128 °C. IR (KBr, *v*, cm^{-1}): 1536 (s, C=N); 1322 (s, NO_2); 1156 (s, C–O–C). ^{13}C NMR (300 MHz, $CDCl_3$, ppm): *δ* 159.7; 153.7 (CH=N); 141.3; 138.9; 137.1; 130.3; 129.2; 128.7; 127.9; 127.3; 125.8; 124.5; 122.7; 122.1; 118.4; 115.7; 111.4; 70.8 (CH_2). ^1H NMR ($CDCl_3$, 300 MHz): 5.35 (t, *J* = 10.52 Hz, 2H); 6.39 (d, *J* = 8.76 Hz, 1H); 7.07 (m, 1H); 7.19 (d, *J* = 7.50 Hz, 1H); 7.32–7.37 (m, 2H); 7.48 (t, *J* = 7.31 Hz, 1H); 8.09 (d, *J* = 2.55 Hz, 1H); 8.48 (d, *J* = 3.12 Hz, 3H). ESI-MS: 558.23 ($C_{21}H_{13}BrF_4N_3O_6$ $[M+H]^+$). Anal. Calcd for $C_{21}H_{12}BrF_4N_3O_6$: C, 45.18; H, 2.17; N, 7.53. Found: C, 45.28; H, 2,15; N, 7.57.

4.3.11. (*E*)-5-Bromo-2-(2,6-dinitro-4-(trifluoromethyl) phenoxy)benzaldehyde *O*-(2-chlorobenzyl) oxime (11h)

Yellow solid, yield 68%, mp: 108–109 °C. IR (KBr, *v*, cm^{-1}): 1546 (s, C=N); 1323 (s, NO_2); 11474 (s, C–O–C). ^{13}C NMR (300 MHz, $CDCl_3$, ppm): *δ* 145.8 (CH=N); 142.5; 134.7; 133.2; 132.0; 130.0; 129.4; 129.2; 127.6; 126.9; 126.7; 126.4; 126.2; 126.1; 126.0; 123.5; 123.3; 119.7; 76.5 (CH_2). ^1H NMR ($CDCl_3$, 300 MHz): 5.39 (s, 2H); 6.39 (d, *J* = 8.85 Hz, 1H); 7.26–7.30 (m, 2H); 7.32–7.36 (m, 1H); 7.4005 (t, *J* = 4.58 Hz, 1H); 7.49 (d, *J* = 6.39 Hz, 1H); 8.08 (d, *J* = 2.40 Hz, 1H); 8.47 (s, 2H); 8.53 (s, 1H). ESI-MS: 574.69 ($C_{21}H_{13}BrClF_3N_3O_6$ $[M+H]^+$). Anal. Calcd for $C_{21}H_{12}BrClF_3N_3O_6$: C, 43.89; H, 2.10; N, 7.31. Found: C, 43.78; H, 2.15; N, 7.38.

4.3.12. (*Z*)-5-Bromo-2-(2,6-dinitro-4-(trifluoromethyl)phenoxy) benzaldehyde *O*-(2,4-dichlorobenzyl) oxime (12h)

Yellow solid, yield 73%, mp: 117–125 °C. IR (KBr, *v*, cm^{-1}): 1546 (s, C=N); 1318 (s, NO_2); 1145 (s, C–O–C). ^{13}C NMR (300 MHz, $CDCl_3$, ppm): *δ* 158.7; 152.7 (CH=N); 142.7; 138.7; 136.7; 136.3; 134.6; 133.8; 131.6; 130.3; 127.3; 127.1; 125.9; 123.3; 122.1; 118.4; 111.0; 71.5 (CH_2). ^1H NMR ($CDCl_3$, 300 MHz): 5.33 (s, 2H); 6.39 (d, *J* = 8.79 Hz, 1H); 7.28 (d, *J* = 10.05 Hz, 1H); 7.33–7.37 (m, 1H); 7.43 (t, *J* = 7.68 Hz, 2H); 8.05 (d, *J* = 3.12 Hz, 1H); 8.44 (d, *J* = 11.88 Hz, 3H). ESI-MS: 609.13 ($C_{21}H_{12}BrCl_2F_3N_3O_6$ $[M+H]^+$). Anal. Calcd for $C_{21}H_{11}BrCl_2F_3N_3O_6$: C, 41.41; H, 1.82; N, 6.90. Found: C, 41.34; H, 1.78; N, 6.97.

4.3.13. 3,5-Dichloro-2-(2,6-dinitro-4-(trifluoromethyl)phenoxy) benzaldehyde *O*-benzyl oxime (13h)

Yellow solid, yield 79%, mp: 139–145 °C. IR (KBr, *v*, cm^{-1}): 1545 (s, C=N); 1317 (s, NO_2); 1143 (s, C–O–C). ^{13}C NMR (300 MHz, $CDCl_3$, ppm): *δ* 161.6; 152.8 (CH=N); 143.2; 139.8; 137.3; 133.8; 130.4; 128.9; 127.1; 125.9; 121.4; 120.9; 120.1; 117.8; 110.4; 76.6 (CH_2). ^1H NMR ($CDCl_3$, 300 MHz): 5.28 (d, *J* = 10.62 Hz, 2H); 6.38 (d, *J* = 8.76 Hz, 1H); 7.26–7.44 (m, 5H); 8.08 (d, *J* = 2.40 Hz, 1H); 8.47 (d, *J* = 6.06 Hz, 3H). ESI-MS: 530.24 ($C_{21}H_{13}Cl_2F_3N_3O_6$ $[M+H]^+$). Anal. Calcd for $C_{21}H_{12}Cl_2F_3N_3O_6$: C, 47.57; H, 2.28; N, 7.92. Found: C, 47.50; H, 2.31; N, 7.89.

4.3.14. 3,5-Dichloro-2-(2,6-dinitro-4-(trifluoromethyl)phenoxy) benzaldehyde *O*-(2-fluorobenzyl) oxime (14h)

Yellow solid, yield 83%, mp: 111–112 °C. IR (KBr, *v*, cm^{-1}): 1547 (s, C=N); 1319 (s, NO_2); 1142 (s, C–O–C). ^{13}C NMR (300 MHz, $CDCl_3$, ppm): *δ* 159.4; 152.7 (CH=N); 147.4; 141.3; 139.8; 132.4; 130.7; 129.2; 128.9; 128.7; 127.6; 127.3; 127.0; 125.9; 124.5; 122.3; 122.1; 115.7; 69.8 (CH_2). ^1H NMR ($CDCl_3$, 300 MHz): 5.28 (t, *J* = 10.10 Hz, 2H); 7.06–7.13 (m, 1H); 7.17 (d, *J* = 7.50 Hz, 1H); 7.30–7.37 (m, 2H); 7.44 (t, *J* = 7.40 Hz, 1H); 7.83 (d, *J* = 2.55 Hz, 1H); 8.29 (s, 2H); 8.39 (s, 1H). ESI-MS: 548.23 ($C_{21}H_{11}Cl_3F_4N_3O_6$ $[M+H]^+$). Anal. Calcd for $C_{21}H_{11}Cl_2F_4N_3O_6$: C, 46.01; H, 2.026; N, 7.66. Found: C, 46.11; H, 2.01; N, 7.66

4.3.15. (*E*)-3,5-Dichloro-2-(2,6-dinitro-4-(trifluoromethyl) phenoxy)benzaldehyde *O*-(2-chlorobenzyl) oxime (15h)

Yellow solid, yield 69%, mp: 154–156 °C. IR (KBr, *v*, cm^{-1}): 1545 (s, C=N); 1318 (s, NO_2); 1150 (s, C–O–C). ^{13}C NMR (300 MHz, $CDCl_3$, ppm): *δ* 153.8 (CH=N); 147.4; 143.3; 139.8; 138.2; 132.4; 130.7; 129.0; 128.9; 128.5; 127.3; 127.0; 125.9; 122.9; 122.1; 70.9 (CH_2). ^1H NMR ($CDCl_3$, 300 MHz): 5.37 (s, 2H); 7.26–7.30 (m, 1H); 7.33 (d, *J* = 2.55 Hz, 1H); 7.39–7.42 (m, 1H); 7.44–7.51 (m, 1H); 7.83 (d, *J* = 2.55 Hz, 1H); 8.30 (s, 2H); 8.44 (s, 1H). ESI-MS: 564.68 ($C_{21}H_{12}Cl_3F_3N_3O_6$ $[M+H]^+$). Anal. Calcd for

$C_{21}H_{11}Cl_3F_3N_3O_6$: C, 44.67; H, 1.96; N, 7.44. Found: C, 44.75; H, 1.99; N, 7.42.

4.3.16. (*E*)-3,5-Dichloro-2-(2,6-dinitro-4-(trifluoromethyl) phenoxy)benzaldehyde *O*-(2,4-dichlorobenzyl) oxime (16h)

Yellow solid, yield 75%, mp: 170–171 °C. IR (KBr, *v*, cm^{-1}): 1543 (s, C=N); 1319 (s, NO_2); 1151 (s, C–O–C). ^{13}C NMR (300 MHz, $CDCl_3$, ppm): δ 154.8 (CH=N); 147.7; 142.3; 139.8; 136.4; 134.6; 133.7; 132.4; 130.6; 129.9; 128.0; 127.3; 127.1; 127.0; 125.9; 122.6; 122.1; 70.5 (CH_2). ^1H NMR ($CDCl_3$, 300 MHz): 5.30 (d, *J* = 9.69 Hz, 2H); 7.26–7.30 (m, 1H); 7.33 (d, *J* = 2.55 Hz, 1H); 7.39–7.44 (m, 1H); 7.46–7.51 (m, 1H); 7.80 (d, *J* = 2.55 Hz, 1H); 8.29 (s, 2H); 8.44 (s, 1H). ESI-MS: 599.13 ($C_{21}H_{11}Cl_4F_3N_3O_6$ $[M+H]^+$). Anal. Calcd for $C_{21}H_{10}Cl_4F_3N_3O_6$: C, 42.10; H, 1.68; N, 7.01. Found: C, 42.03; H, 1.69; N, 7.61.

4.3.17. 3,5-Dibromo-2-(2,6-dinitro-4-(trifluoromethyl) phenoxy)benzaldehyde *O*-benzyl oxime (17h)

Yellow solid, yield 79%, mp: 123–124 °C. IR (KBr, *v*, cm^{-1}): 1544 (s, C=N); 1315 (s, NO_2); 1141 (s, C–O–C). ^{13}C NMR (300 MHz, $CDCl_3$, ppm): δ 153.8 (CH=N); 147.7; 144.6; 142.5; 136.7; 133.7; 129.2; 128.9; 128.1; 126.9; 126.6; 126.1; 126.0; 119.8; 112.1; 76.9 (CH2). ^1H NMR ($CDCl_3$, 300 MHz): 5.12 (s, 2H); 7.28–7.37 (m, 5H); 7.90 (d, *J* = 2.19 Hz, 1H); 8.07 (d, *J* = 2.4 Hz, 1H); 8.41 (s, 1H); 8.83 (s, 2H). ESI-MS: 619.14 ($C_{21}H_{13}Br_2F_3N_3O_6$ $[M+H]^+$). Anal. Calcd for $C_{21}H_{12}Br_2F_3N_3O_6$: C, 40.74; H, 1.95; N, 6.79. Found: C, 40.83; H, 1.99; N, 6.76.

4.3.18. 3,5-Dibromo-2-(2,6-dinitro-4-(trifluoromethyl) phenoxy)benzaldehyde *O*-(2-fluorobenzyl) oxime (18h)

Yellow solid, yield 88%, mp: 94–96 °C. IR (KBr, *v*, cm^{-1}): 1548 (s, C=N); 1316 (s, NO_2); 1144 (s, C–O–C). ^{13}C NMR (300 MHz, $CDCl_3$, ppm): δ 162.5; 159.2 (CH=N); 147.3; 142.5; 130.6; 130.5; 130.0; 129.9; 128.0; 126.9; 126.7; 126.2; 126.1; 126.0; 124.0; 123.9; 123.8; 119.8; 119.7; 115.5; 115.2; 112.1; 70.6 (CH_2). ^1H NMR ($CDCl_3$, 300 MHz): 5.23 (d, *J* = 37.32 Hz, 2H); 7.15–7.23 (m, 2H); 7.36–7.43 (m, 2H); 7.95 (d, *J* = 2.37 Hz, 1H); 8.07 (d, *J* = 2.40 Hz, 1H); 8.41 (s, 1H); 8.83 (s, 2H). ESI-MS: 637.13 ($C_{21}H_{12}Br_2F_4N_3O_6$ $[M+H]^+$). Anal. Calcd for $C_{21}H_{11}Br_2F_4N_3O_6$: C, 39.59; H, 1.74; N, 6.60. Found: C, 39.51; H,1.74; N, 6.63.

4.3.19. 3,5-Dibromo-2-(2,6-dinitro-4-(trifluoromethyl) phenoxy)benzaldehyde *O*-(2-chlorobenzyl) oxime (19h)

Yellow solid, yield 75%, mp: 112–114 °C. IR (KBr, *v*, cm^{-1}): 1550 (m, C=N); 1339 (m, NO_2); 1167 (s, C–O–C). ^{13}C NMR (300 MHz, $CDCl_3$, ppm): δ 163.7; 153.6 (CH=N); 141.4, 137.8; 136.3; 133.8; 132.7; 128.6; 127.5; 125.9; 121.6; 120.9; 120.4; 117.6; 110.6; 77.5(CH_2). ^1H NMR ($CDCl_3$, 300 MHz): 5.35 (d, *J* = 9.51 Hz, 2H); 6.45 (d, *J* = 8.76 Hz, 1H); 7.19–7.23 (m, 1H); 7.28 (t, *J* = 5.04 Hz, 1H); 7.43 (t, *J* = 3.93 Hz, 2H); 7.90 (d, *J* = 2.73 Hz, 1H); 8.47 (s, 2H); 8.52 (s, 1H). ESI-MS: 653.58 ($C_{21}H_{12}Br_2ClF_3N_3O_6$ $[M+H]^+$). Anal. Calcd for $C_{21}H_{11}Br_2ClF_3N_3O_6$: C, 38.59; H, 1.70; N, 6.43. Found: C, 38.65; H, 1.56; N, 6.37.

4.3.20. (*E*)-3,5-Dibromo-2-(2,6-dinitro-4-(trifluoromethyl) phenoxy)benzaldehyde *O*-(2,4-dichlorobenzyl) oxime (20h)

Yellow solid, yield 66%, mp: 157–159 °C. IR (KBr, *v*, cm^{-1}): 1547 (s, C=N); 1323 (s, NO_2); 1145 (s, C–O–C). ^{13}C NMR (300 MHz, $CDCl_3$, ppm): δ 161.5; 152.8 (CH=N); 142.7; 138.3; 137.3; 133.7; 130.4; 127.9; 127.1; 125.6; 121.9; 120.8; 120.1; 119.8; 111.8; 76.3 (CH_2). ^1H NMR1H NMR($CDCl_3$, 300 MHz): 7.24 (s, 1H); 7.36 (t, *J* = 9.61 Hz, 1H); 7.41–7.44 (m, 2H); 7.64 (t, *J* = 2.28 Hz, 2H); 7.97 (d, *J* = 2.19 Hz, 1H); 8.27 (s, 2H); 8.41 (s, 1H). ESI-MS: 688.03 ($C_{21}H_{11}Br_2Cl_2F_3N_3O_6$ $[M+H]^+$). Anal. Calcd for $C_{21}H_{10}Br_2Cl_2F_3N_3O_6$: C, 36.66; H, 1.46; N, 6.11. Found: C, 36.73; H, 1.48; N, 6.07.

4.4. Crystal structure determination

Crystal structure determination of compound **4h** were carried out on a Nonius CAD4 diffractometer equipped with graphite-monochromated Mo Ka (*k* = 0.71073 Å) radiation (Fig. 3). The structure was solved by direct methods and refined on F^2 by full-matrix least-squares methods using SHELX-97.[28] All non-hydrogen atoms of compound **4h** were refined with anisotropic thermal parameters. All hydrogen atoms were placed in geometrically idealized positions and constrained to ride on their parent atoms. The crystal data, data collection and refinement parameters for the compound **4h** are listed in Table 2.

4.5. Antiproliferation assay

The antiproliferative activities of the prepared compounds against MCF-7, Hep-G2 and A549 cells were evaluated as described in the literature[29] with some modifications. Target tumor cell lines were grown to log phase in RPMI 1640 medium supplemented with 10% fetal bovine serum. After diluting to 2×10^4 cells mL^{-1} with the complete medium, 100 μL of the obtained cell suspension was added to each well of 96-well culture plates. The subsequent incubation was permitted at 37 °C, 5% CO_2 atmosphere for 24 h before the cytotoxicity assessments. Tested samples at pre-set concentrations were added to six wells with colchicines and CA-4 co-assayed as positive references. After 48 h exposure period, 40 μL of PBS containing 2.5 mg mL^{-1} of MTT (3-(4,5-dimethylthiazol-2-yl)-2,5-diphenyltetrazolium bromide)) was added to each well. Four hours later, 100 μL extraction solution (10% SDS–5% isobutyl alcohol–0.01 M HCl) was added. After an overnight incubation at 37 °C, the optical density was measured at a wavelength of 570 nm on an ELISA microplate reader. In all experiments three replicate wells were used for each drug concentration. Each assay was carried out for at least three times. The results were summarized in Table 3.

4.6. Effects on tubulin polymerization

Bovine brain tubulin was purified as described previously.[30] To evaluate the effect of the compounds on tubulin assembly in vitro,[31] varying concentrations were preincubated with 10 μM tubulin in glutamate buffer at 30 °C and then cooled to 0 °C. After addition of GTP, the mixtures were transferred to 0 °C cuvettes in a recording spectrophotometer and warmed up to 30 °C and the assembly of tubulin was observed turbid metrically. The IC_{50} was defined as the compound concentration that inhibited the extent of assembly by 50% after 20 min incubation.

4.7. Apoptosis assay

MCF-7 cells were cultured with various concentrations of compounds for 24 h. Then, the cells were harvested and stained with both Annexin V-FITC (fluorescein isothiocyanate) and PI (propidium iodide) for 20 min. The samples were analyzed by flow cytometer (FCM).

4.8. Docking simulations

The crystal structure of tubulin (PDB code: 1SA0)[10,32] was obtained from the RCSB Protein Data Bank (http://www.rcsb.org/pdb/home/home.do). The molecular docking procedure was performed by using LigandFit protocol within Discovery Studio 3.1. For ligand preparation, the 3D structures of **2h** were generated and minimized using Discovery Studio 3.1. For protein preparation, the hydrogen atoms were added, and the water and impurities were removed. The whole tubulin was defined as a receptor and

the site sphere was selected based on the ligand binding location of colchicine, then the colchicine molecule was removed and **2h** was placed during the molecular docking procedure. Types of interactions of the docked protein with ligand were analyzed after the end of molecular docking.

Acknowledgment

This work was financed by National Natural Science Foundation of China (No. J1103512).

References and notes

1. Frace, A.; Loge, C.; Gallet, S.; Lebegue, N.; Carato, P.; Chavatte, P.; Berthelot, P.; Lesieur, D. J. *Enzyme Inhib. Med. Chem.* **2004**, *19*, 541.
2. Kanthou, C.; Tozer, G. M. *Int. J. Exp. Pathol.* **2009**, *90*, 284.
3. De Rycker, M.; Rigoreau, L.; Dowding, S.; Parker, P. J. *Chem. Biol. Drug Des.* **2009**, *73*, 599.
4. Hait, W. N.; Hambley, T. W. *Cancer Res.* **2009**, *69*, 1263.
5. Pellegrini, F.; Budman, D. R. *Cancer Invest.* **2005**, *23*, 264.
6. Ravelli, R. B.; Gigant, B.; Curmi, P. A.; Jourdain, I.; Lachkar, S.; Sobel, A.; Knossow, M. *Nature* **2004**, *428*, 198.
7. Simoni, D.; Romagnoli, R.; Baruchello, R.; Rondanin, R.; Rizzi, M.; Pavani, M. G.; Alloatti, D.; Giannini, G.; Marcellini, M.; Riccioni, T.; Castorina, M.; Guglielmi, M. B.; Bucci, F.; Carminati, P.; Pisano, C. *J. Med. Chem.* **2006**, *49*, 3033.
8. Zhou, J.; Giannakakou, P. *Curr. Med. Chem.* **2005**, *5*, 10.
9. Carlson, R. O. *Expert Opin. Invest. Drugs* **2008**, *17*, 707.
10. Alberto, M.; Sewan, T.; Ornella, M.; Antonio, C.; Armando, A. G.; Gian, C. T. *Chem. Biol. Drug. Des.* **2011**, *78*, 913.
11. Pascal, V. P.; Garès, M.; Michel, W. *Biochem. Pharmacol.* **1999**, *59*, 959.
12. Kozurkova, M.; Sabolova, D.; Paulikova, H.; Janovec, L.; Kristian, P.; Bajdichova, M.; Busa, J.; Pldhradsky, D.; Imrich, J. *Int. J. Biol. Macromol.* **2007**, *41*, 415.
13. Foroumadi, A.; Emami, S.; Rajabalian, S. *Biomed. Pharmacother.* **2009**, *63*, 216.
14. Cashman, D. J.; Kellogg, G. E. *J. Med. Chem.* **2004**, *47*, 1360.
15. Kuz'min, V. E.; Artemenko, A. G.; Lozytska, R. N.; Fedtchouk, A. S.; Lozitsky, V. P.; Muratov, E. N.; Mescheriakov, A. K. *SAR QSAR Environ. Res.* **2005**, *16*, 219.
16. Shekawat, D. R.; Sabnis, S. S.; Deliwala, C. V. *J. Med. Chem.* **1972**, *15*, 1196.
17. Nasser, M. H.; Yousery, E. S.; Amany, A. E. R. *J. Coord. Chem.* **2008**, *61*, 2536.
18. Nilufer, S.; Sevim, R. *ARKIVOC* **2006**, *12*, 173.
19. Aliasghar, J.; Dariush, K.; Erik, D. C.; Chanaz, S.; Jean, M. B. *Molecules* **2007**, *12*, 1720.
20. Samadhiya, S.; Halve, A. *Orient. J. Chem.* **2001**, *17*, 119.
21. Rylan, J. L.; Mark, S. *Angew. Chem., Int. Ed.* **2010**, *49*, 9322.
22. Carmen, L.; Mariana, C. C. *Int. J. Mol. Sci.* **2011**, *12*, 6432.
23. Filler, R.; Saha, R. *Future Med. Chem.* **2009**, *1*, 777.
24. Saeed, A.; Shaheen, U.; Hameed, A.; Haider Naqvi, S. Z. *J. Fluorine Chem.* **2009**, *130*, 1028.
25. Suresh, K. R.; Emil, M.; Iraida, G. S.; Poonam, R. M.; Wang, X. P.; Raymond, J.; Ferid, M.; Rakesh, K. *Proc. Natl. Acad. Sci. U.S.A.* **2007**, *104*, 19470.
26. Reddy, M. A.; Nishant, J. D.; Yada, C. K.; Vangala, J. R.; Reddy, P. S.; Anthony, A.; Shasi, V. K.; Bojja, S. *J. Med. Chem.* **2011**, *54*, 6751.
27. Robert, F.; Rituparna, S. *Future Med. Chem.* **2009**, *1*, 777.
28. Sheldrick, G. M. SHELX-97. Program for X-ray Crystal Structure Solution and Refinement; Göttingen University: Germany, **1997**.
29. Boumendjel, A.; Boccard, J.; Carrupt, P.-A.; Nicolle, E.; Blanc, M.; Geze, A.; Choisnard, L.; Wouessidjewe, D.; Matera, E. L.; Dumontet, C. *J. Med. Chem.* **2008**, *51*, 2307.
30. Hamel, E.; Lin, C. M. *Biochemistry.* **1984**, *23*, 4173.
31. Hamel, E. *Cell Biochem. Biophys.* **2003**, *38*, 1.
32. Luo, Y.; Qiu, K.-M.; Lu, X.; Liu, K.; Fu, J.; Zhu, H.-L. *Bioorg. Med. Chem.* **2011**, *06*, 088.